A Novel Unequal Lumped-Element Coupler With Arbitrary Phase Differences and Arbitrary Impedance Matching

Zhuoyin Chen, Yongle Wu, *Senior Member, IEEE*, Yuhao Yang, and Weimin Wang, *Senior Member, IEEE*

***Abstract*—In this brief, for the first time, a novel compact lumped-element coupler is proposed, which can implement arbitrary power-dividing ratios, arbitrary phase differences, and arbitrary impedance matching. In the design, the proposed coupler is composed of eight lumped LC elements, which achieves a compact circuit size and avoids the complexity of implementation. In the section of circuit analysis, explicit close-formed design equations are derived. For demonstration, three cases of normal couplers and two cases of rat-race couplers extracted from the design procedure are simulated and fabricated. Good agreements between the measurements and simulations verify the design theory of the multifunctional LC coupler.**

***Index Terms*—Arbitrary phase differences, arbitrary power-dividing ratios, arbitrary terminated impedances, coupler, lumped elements, rat-race coupler.**

I. Introduction

COUPLER is one of the most important components in radio frequency (RF)/microwave systems, which can be applied in mixers, power amplifiers, phase shifters, and beamforming antenna arrays. Extensive researches about coupler have been proposed with multifunction in order to meet new requirements, including arbitrary output power division [1]–[9], multiband or wideband [6], [9]–[19], size reduction [3]–[8], [16], impedance transforming [1]–[3], [5], and arbitrary output phase differences [1], [3], [7]. By function, coupler can be classified into many types, such as directional couplers [1], [3]–[9], rat-race couplers [1], [2], [10], and crossovers [18]. According to the division of components of the circuit model, it can be divided into distributed-element couplers [1], [2], [6]–[9], and lumped-element couplers [3]–[5], [16]–[20]. The distributed couplers have been studied extensively. An unequal branch-line coupler with arbitrary phase differences, and arbitrary I/O impedances is proposed in [1], and the supplementary explanation of the multifunctional rat-race coupler is in [2]. In addition, coupler can be fabricated with PCB [1], [8]–[13], SMD [4], [5], CMOS [16], MMIC [3], [17], and low-temperature co-fired ceramic (LTCC) [19] technology.

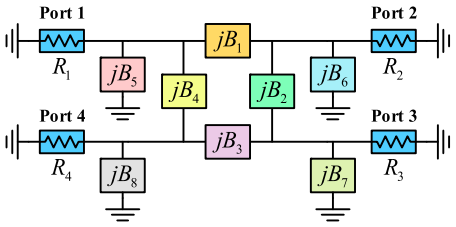

Fig. 1. The circuit model of the proposed lumped-element coupler.

However, the distributed components occupy a large area on the circuit board, which hinder the size reduction, especially in microwave integrated circuits at low frequencies (below 20 GHz). The use of lumped-element components can reduce the size and decrease manufacturing complexity, in line with the trend of miniaturization. There is no specific topology structural limitation for designing the lumped-element couplers. In [3], the design of lumped-element coupler is described with arbitrary power division and impedance transformation between the input and output in MIC and MMIC applications. In [5], an unequal lumped-element coupler is presented with impedance transformation based on the replacement of branch-line coupler using Pi-type network. Designing a compact lumped-element coupler with arbitrary power-dividing ratios and arbitrary phase difference is proposed [4]. Using LTCC technology, a wideband lumped-element rat-race coupler is designed [19]. However, a lumped-element coupler with arbitrary power-dividing ratios, arbitrary phase differences, and arbitrary terminated impedances has not been proposed, and the corresponding design method using lumped elements has not been presented in the previous work.

In this brief, a lumped-element coupler with arbitrary power-dividing ratios (between through and coupled ports), arbitrary phase differences (including rat-race case), and arbitrary impedance matching is proposed for the first time, which only uses eight LC components. The basic topology is inspired by the branch-line coupler [1] and lumped-element directional couplers [3]. Eight susceptance modules constitute a new lumped-element coupler, which provide sufficient design flexibility. The closed-form design equations are derived. The design equations are appropriated for the phase difference ranging from 0° to 360° (−180° to +180°), including

Manuscript received February 9, 2021; revised May 10, 2021; accepted June 22, 2021. Date of publication June 30, 2021; date of current version January 31, 2022. This work was supported in part by the National Natural Science Foundations of China under Grant U20A20203 and Grant 61971052; and in part by the Beijing Natural Science Foundation under Grant JQ19018. This brief was recommended by Associate Editor Y. Qin. *(Corresponding authors: Yongle Wu; Weimin Wang.)*

The authors are with the School of Electronic Engineering, Beijing University of Posts and Telecommunications, Beijing 100876, China (e-mail: chenzhuoyin001@gmail.com; wuyongle138@gmail.com; yangyuhao1996@gmail.com; wangwm@bupt.edu.cn).

Color versions of one or more of the figures in this paper are available online at https://doi.org/10.1109/TCSII.2021.3093528.

Digital Object Identifier 10.1109/TCSII.2021.3093528

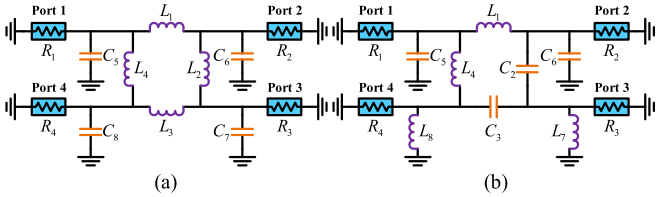

Fig. 2. Schematics of the LC couplers. (a) *Case A* & *Case C*. (b) *Case B*.

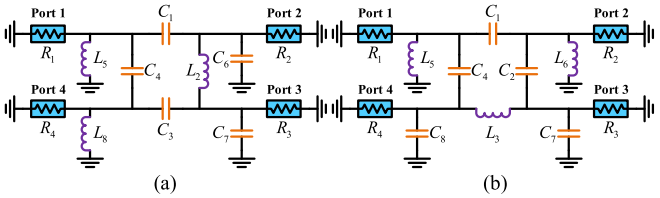

Fig. 3. Schematics of the LC rat-race couplers. (a) *Case D*. (b) *Case E*.

the case of the rat-race coupler. Finally, compared to the previous designs [1], [4], the proposed coupler has the advantages of the simple circuit structure and design procedure, easy implementation, arbitrary power-dividing ratios, arbitrary phase differences, and good arbitrary terminated impedance matching.

II. Circuit Structure & Design Equations

The circuit model of the proposed unequal LC coupler with arbitrary phase differences and arbitrary impedances matching is shown in Fig. 1. In this model, there is a lumped component connection between port 1 and 2, 2 and 3, 3 and 4, 4 and 1, which can be expressed as B_1, B_2, B_3, and B_4. Each port and ground are connected with a lumped component, which is B_5, B_6, B_7, and B_8. Terminated impedance of the four ports can be expressed as R_1, R_2, R_3, and R_4, which are the real numbers. The eight admittance components can be expressed as $Y_i = jB_i$, and the susceptance B_i can be defined as

$$B_i = \begin{cases} \omega C_i, & 0 < B_i < \infty \\ open, & B_i = 0 \\ -\frac{1}{\omega L_i}, & -\infty < B_i < 0 \\ short, & B_i = \pm\infty, \end{cases} \tag{1}$$

where i = 1, 2, …, 8.

Starting from the Y-parameter definition, according to the circuit model, Y-matrix of the coupler can be expressed as

$$Y_{circuit} = \begin{pmatrix} jB_5 + jB_4 + jB_1 & -jB_1 & 0 & -jB_4 \\ -jB_1 & jB_6 + jB_1 + jB_2 & -jB_2 & 0 \\ 0 & -jB_2 & jB_7 + jB_2 + jB_3 & -jB_3 \\ -jB_4 & 0 & -jB_3 & jB_8 + jB_3 + jB_4 \end{pmatrix}. \tag{2}$$

A. Phase Difference Not Equal to 0° or 180° (Normal Case)

With the normal coupler definition, port 1 is the input port, port 2 is the through port, port 3 is the coupled port, and port 4 is the isolated port. Therefore, the expected S-matrix can be discussed. Assuming that the phases of S_{12} and S_{34} are $\psi_{1,2}$, the phase difference is Φ, and the power-dividing ratio is $k^2 = |S_{21} / S_{31}|^2$, the expected S-matrix can be expressed as

$$S_{expected} = \begin{pmatrix} 0 & \frac{ke^{j\psi_1}}{\sqrt{k^2+1}} & \frac{e^{j(\psi_1-\phi)}}{\sqrt{k^2+1}} & 0 \\ \frac{ke^{j\psi_1}}{\sqrt{k^2+1}} & 0 & 0 & \frac{e^{j(\pi+\psi_2+\phi)}}{\sqrt{k^2+1}} \\ \frac{e^{j(\psi_1-\phi)}}{\sqrt{k^2+1}} & 0 & 0 & \frac{ke^{j\psi_2}}{\sqrt{k^2+1}} \\ 0 & \frac{e^{j(\pi+\psi_2+\phi)}}{\sqrt{k^2+1}} & \frac{ke^{j\psi_2}}{\sqrt{k^2+1}} & 0 \end{pmatrix}. \tag{3}$$

Due to the circuit characteristic is denoted by Y-matrix, the expected S-matrix needs to be converted to Y-matrix. The expected Y-matrix is calculated as [1]

$$Y_{expected} = \begin{pmatrix} \frac{j\cot\phi}{R_1} & \mp\frac{j\sqrt{k^2+1}\csc\phi}{k\sqrt{R_1R_2}} & 0 & \mp\frac{j\csc\phi}{k\sqrt{R_1R_4}} \\ \mp\frac{j\sqrt{k^2+1}\csc\phi}{k\sqrt{R_1R_2}} & \frac{j\cot\phi}{R_2} & \frac{j\csc\phi}{k\sqrt{R_2R_3}} & 0 \\ 0 & \frac{j\csc\phi}{k\sqrt{R_2R_3}} & -\frac{j\cot\phi}{R_3} & \frac{j\sqrt{k^2+1}\csc\phi}{k\sqrt{R_3R_4}} \\ \mp\frac{j\csc\phi}{k\sqrt{R_1R_4}} & 0 & \frac{j\sqrt{k^2+1}\csc\phi}{k\sqrt{R_3R_4}} & -\frac{j\cot\phi}{R_4} \end{pmatrix}, \tag{4}$$

where the upper and lower signs represent $\psi_1 = \Phi$ and $\psi_1 = \Phi + \pi$, respectively.

The coupler circuit needs to be worked as expected, so the equation is $Y_{\text{circuit}} = Y_{\text{expected}}$. Through this equation, all eight admittance parameters are calculated as (5), where the upper and lower signs represent $\psi_1 = \Phi$ and $\psi_1 = \Phi + \pi$, respectively. The choice of ψ_1 requires consideration of circuit performance, which will be discussed in Section III-A.

$$B_1 = \pm\frac{\sqrt{k^2+1}\csc\phi}{k\sqrt{R_1R_2}}, B_2 = -\frac{\csc\phi}{k\sqrt{R_2R_3}}, \tag{5a}$$

$$B_3 = -\frac{\sqrt{k^2+1}\csc\phi}{k\sqrt{R_3R_4}}, B_4 = \pm\frac{\csc\phi}{k\sqrt{R_1R_4}}, \tag{5b}$$

$$B_5 = \frac{\cot\phi}{R_1} \mp \frac{\csc\phi}{k\sqrt{R_1R_4}} \mp \frac{\sqrt{k^2+1}\csc\phi}{k\sqrt{R_1R_2}}, \tag{5c}$$

$$B_6 = \frac{\cot\phi}{R_2} \mp \frac{\sqrt{k^2+1}\csc\phi}{k\sqrt{R_1R_2}} + \frac{\csc\phi}{k\sqrt{R_2R_3}}, \tag{5d}$$

$$B_7 = -\frac{\cot\phi}{R_3} + \frac{\csc\phi}{k\sqrt{R_2R_3}} + \frac{\sqrt{k^2+1}\csc\phi}{k\sqrt{R_3R_4}}, \tag{5e}$$

$$B_8 = -\frac{\cot\phi}{R_4} + \frac{\sqrt{k^2+1}\csc\phi}{k\sqrt{R_3R_4}} \mp \frac{\csc\phi}{k\sqrt{R_1R_4}}. \tag{5f}$$

B. Phase Difference Equal to 0° or 180° (the Rat-Race Case)

With the rat-race coupler definition, port 1 is the input port, port 2 is the through port, port 4 is the coupled port, and port 3 is the isolated port. The output ports will be in-phase when port 1 is excited, the output ports will be the anti-phase when port 3 is excited. Similar to the above, the expected S-matrix and Y-matrix can be expressed as (6) and (7), where the upper and lower signs represent $\psi_2 = \psi_1$ and $\psi_2 = \psi_1 + \pi$, respectively.

$$S_{expected} = \begin{pmatrix} 0 & \frac{ke^{j\psi_1}}{\sqrt{k^2+1}} & 0 & \frac{e^{j\psi_1}}{\sqrt{k^2+1}} \\ \frac{ke^{j\psi_1}}{\sqrt{k^2+1}} & 0 & \frac{e^{j(\psi_2+\pi)}}{\sqrt{k^2+1}} & 0 \\ 0 & \frac{e^{j(\psi_2+\pi)}}{\sqrt{k^2+1}} & 0 & \frac{ke^{j\psi_2}}{\sqrt{k^2+1}} \\ \frac{e^{j\psi_1}}{\sqrt{k^2+1}} & 0 & \frac{ke^{j\psi_2}}{\sqrt{k^2+1}} & 0 \end{pmatrix}, \tag{6}$$

TABLE I
PARAMETER VALUES OF THE GENERALIZED CASES

	Case A	*Case B*	*Case C*	*Case D*	*Case E*
k (dB)	4	0	3	0	3
ψ_1 (°) / ψ_2 (°)	Φ (60) + 180	Φ (250)	Φ (130) + 180	ψ_1 (80)	ψ_1 (85) + 180
R_1 (Ω)	50	42	50	50	50
R_2 (Ω)	50	50	75	45	50
R_3 (Ω)	50	60	60	42	50
R_4 (Ω)	50	75	100	60	50
L_1 (nH) / C_1 (pF)	5.83 (nH)	4.85 (nH)	6.09 (nH)	2.41 (pF)	2.61 (pF)
L_2 (nH) / C_2 (pF)	10.92 (nH)	3.09 (pF)	11.55 (nH)	9.64 (nH)	1.85 (pF)
L_3 (nH) / C_3 (pF)	5.83 (nH)	3.57 (pF)	7.71 (nH)	2.28 (pF)	9.71 (nH)
L_4 (nH) / C_4 (pF)	10.92 (nH)	8.39 (nH)	12.18 (nH)	2.09 (pF)	1.85 (pF)
L_5 (nH) / C_5 (pF)	8.50 (pF)	9.62 (pF)	3.57 (pF)	6.44 (nH)	6.07 (nH)
L_6 (nH) / C_6 (pF)	8.50 (pF)	3.29 (pF)	4.57 (pF)	0.84 (pF)	6.07 (nH)
L_7 (nH) / C_7 (pF)	4.83 (pF)	3.32 (nH)	7.70 (pF)	1.02 (pF)	1.04 (pF)
L_8 (nH) / C_8 (pF)	4.83 (pF)	19.11 (nH)	6.70 (pF)	6.50 (nH)	1.04 (pF)

The rat-race coupler needs to be worked as expected, which is $Y_{\text{circuit}} = Y_{\text{expected}}$. Through this equation, all eight admittance parameters are calculated as (8), where the upper and lower signs represent $\psi_2 = \psi_1$ and $\psi_2 = \psi_1 + \pi$, respectively. The choice of ψ_2 requires consideration of circuit performance.

$$Y_{expected} = \begin{pmatrix} \frac{j\cot\psi_1}{R_1} & -\frac{jk\csc\psi_1}{\sqrt{R_1R_2}\sqrt{k^2+1}} & 0 & -\frac{j\csc\psi_1}{\sqrt{R_1R_4}\sqrt{k^2+1}} \\ -\frac{jk\csc\psi_1}{\sqrt{R_1R_2}\sqrt{k^2+1}} & \frac{j\cot\psi_1}{R_2} & \pm\frac{j\csc\psi_1}{\sqrt{R_2R_3}\sqrt{k^2+1}} & 0 \\ 0 & \pm\frac{j\csc\psi_1}{\sqrt{R_2R_3}\sqrt{k^2+1}} & \frac{j\cot\psi_1}{R_3} & \mp\frac{jk\csc\psi_1}{\sqrt{R_3R_4}\sqrt{k^2+1}} \\ -\frac{j\csc\psi_1}{\sqrt{R_1R_4}\sqrt{k^2+1}} & 0 & \mp\frac{jk\csc\psi_1}{\sqrt{R_3R_4}\sqrt{k^2+1}} & \frac{j\cot\psi_1}{R_4} \end{pmatrix}. \tag{7}$$

$$B_1 = \frac{k\csc\psi_1}{\sqrt{R_1R_2}\sqrt{k^2+1}}, B_2 = \mp\frac{\csc\psi_1}{\sqrt{R_2R_3}\sqrt{k^2+1}}, \tag{8a}$$

$$B_3 = \pm\frac{k\csc\psi_1}{\sqrt{R_3R_4}\sqrt{k^2+1}}, B_4 = \frac{\csc\psi_1}{\sqrt{R_1R_4}\sqrt{k^2+1}}, \tag{8b}$$

$$B_5 = \frac{\cot\psi_1}{R_1} - \frac{\csc\psi_1}{\sqrt{R_1R_4}\sqrt{k^2+1}} - \frac{k\csc\psi_1}{\sqrt{R_1R_2}\sqrt{k^2+1}}, \tag{8c}$$

$$B_6 = \frac{\cot\psi_1}{R_2} - \frac{k\csc\psi_1}{\sqrt{R_1R_2}\sqrt{k^2+1}} \pm \frac{\csc\psi_1}{\sqrt{R_2R_3}\sqrt{k^2+1}}, \tag{8d}$$

$$B_7 = \frac{\cot\psi_1}{R_3} \pm \frac{\csc\psi_1}{\sqrt{R_2R_3}\sqrt{k^2+1}} \mp \frac{k\csc\psi_1}{\sqrt{R_3R_4}\sqrt{k^2+1}}, \tag{8e}$$

$$B_8 = \frac{\cot\psi_1}{R_4} \mp \frac{k\csc\psi_1}{\sqrt{R_3R_4}\sqrt{k^2+1}} - \frac{\csc\psi_1}{\sqrt{R_1R_4}\sqrt{k^2+1}}. \tag{8f}$$

III. DESIGN PROCEDURE

A. Normal Coupler

According to (5), the value of ψ_1 can be chosen by $\psi_1 = \Phi$ and $\psi_1 = \Phi + \pi$. The choice of ψ_1 requires consideration of circuit performance. Considering that there are different performances, a set of termination conditions are presented as follows.

1) Parameter values of the capacitor and inductor. The values of the capacitance and inductance need to be selected at a reasonable order of magnitude.

2) Performance requirement. The fractional bandwidth of the S-parameters, the smoothness of the phase difference, and the four port impedances should be suitable for the specific needs.

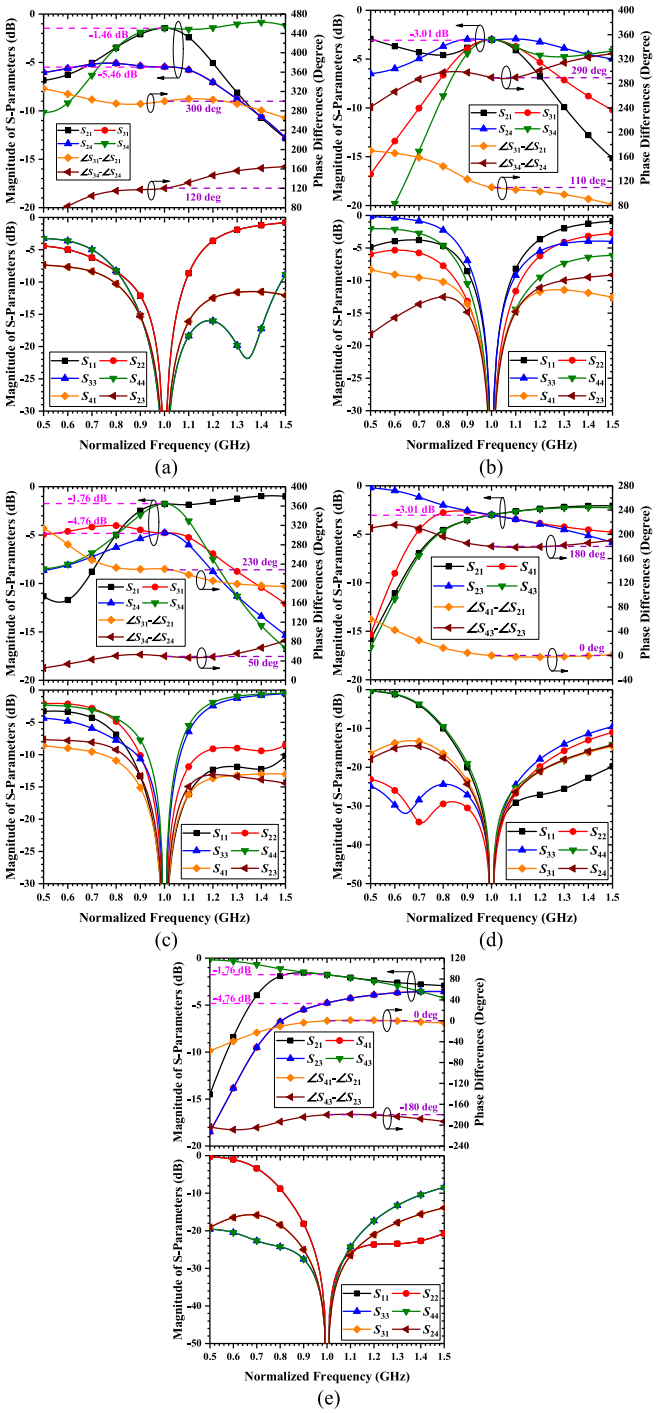

Fig. 4. Calculated ideal S-parameters and phase differences. (a) *Case A*. (b) *Case B*. (c) *Case C*. (d) *Case D*. (e) *Case E*.

In summary, the design procedure of the LC normal coupler (phase difference not equal to 0° or 180°) is listed as follows.

1) *Step 1:* Designate the values of Φ, k, and $R_{1,2,3,4}$ according to the requirements.

2) *Step 2:* Value ψ_1 has two choices, $\psi_1 = \Phi$ and $\psi_1 = \Phi + \pi$. Based on the choice of ψ_1, choose either group of signs for (5) to calculate $B_{1,\ldots,8}$ under different values of ψ_1.

3) *Step 3:* Choose one of the results which is more consistent with the requirements, and then extract the final $B_{1,\ldots,8}$.

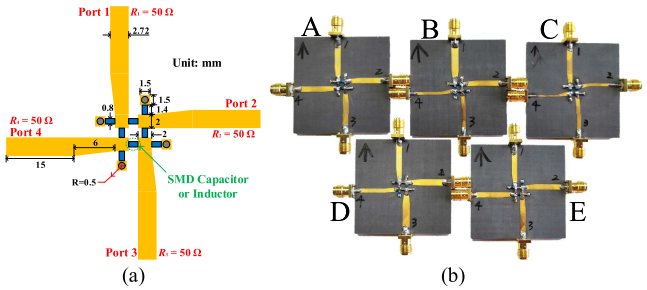

Fig. 5. (a) Layout of the proposed coupler (*Case A*). (b) Photographs of the five fabricated LC couplers.

TABLE II
SIMULATED AND MEASURED PARAMETER VALUES (SIM. / MEA.)

	Case A	*Case B*	*Case C*	*Case D*	*Case E*
L_1 (nH) / C_1 (pF)	3.7 / 4.7(nH)	3.4 / 4.3(nH)	4.8 / 4.7(nH)	2.2 / 2.2(pF)	2.4 / 2.4(pF)
L_2 (nH) / C_2 (pF)	8.5 / 8.7(nH)	2.1 / 3.0(pF)	10.4/10.0(nH)	8.3 / 9.5(nH)	1.7 / 1.8(pF)
L_3 (nH) / C_3 (pF)	3.7 / 4.3(nH)	2.8 / 3.3(pF)	6.3 / 6.2(nH)	2.1 / 2.2(pF)	8.2 / 9.1(nH)
L_4 (nH) / C_4 (pF)	8.5 / 8.7(nH)	6.0 / 7.5(nH)	11.0/11.0(nH)	1.9 / 2.0(pF)	1.7 / 1.8(pF)
L_5 (nH) / C_5 (pF)	6.4 / 6.0(pF)	6.7 / 6.0(pF)	2.9 / 3.0(pF)	5.4 / 6.8(nH)	4.8 / 5.6(nH)
L_6 (nH) / C_6 (pF)	6.4 / 7.0(pF)	2.8 / 3.0(pF)	3.6 / 3.6(pF)	0.8/0.75(pF)	4.6 / 5.6(nH)
L_7 (nH) / C_7 (pF)	3.8 / 3.9(pF)	2.3 / 2.2(nH)	5.6 / 5.6(pF)	1.2 / 1.0(pF)	0.8 / 1.0(pF)
L_8 (nH) / C_8 (pF)	3.8 / 3.9(pF)	14.6/15.0(nH)	5.0 / 5.0(pF)	5.1 / 5.6(nH)	1.0 / 1.0(pF)

B. Rat-Race Coupler

According to (8), the value of ψ_2 can be chosen by $\psi_2 = \psi_1$ and $\psi_2 = \psi_1 + \pi$, and the choice of values for ψ_1 is arbitrary. The choice of ψ_1 requires consideration of circuit performance. The termination conditions are the same as the above. The design procedure of the LC rat-race coupler is listed as follows.

1) *Step 1:* Designate the values of ψ_2 (ψ_1 or $\psi_1 + \pi$), k, and $R_{1,2,3,4}$ according to the requirements.

2) *Step 2:* Select the value of ψ_1. Choose either group of signs for (8) to calculate $B_{1,\ldots,8}$ based on the choice of ψ_1.

3) *Step 3:* If the result based on $B_{1,\ldots,8}$ does not fit the termination conditions, then repeat Steps 2 and 3.

IV. DISCUSSION & EXPERIMENTAL VERIFICATION

To validate the design theory above, three examples of normal couplers (*Case A*, *B*, and *C*) and two examples of rat-race couplers (*Case D* and *E*) are given. The center frequency of all examples is 1 GHz. The configurations of the circuit parameters are listed in Table I. Fig. 2 and Fig. 3 shows the schematics. Fig. 4 show the ideal performances.

The simulations and optimizations are performed by ANSYS HFSS. The designed prototypes are fabricated and measured on F4B substrate ($\varepsilon_r = 2.65$, $h = 1$mm). MuRata capacitors and inductors are used for building the circuits. The simulated and measured values of the capacitors and inductors are listed in Table II. Fig. 5 shows the corresponding circuit layout and photographs of the fabricated LC coupler. The core circuit size of the five couplers is about 11.2 mm $\times$ 11.2 mm ($0.061\lambda_g \times 0.061\lambda_g$). The measured results are obtained by the four-port vector network analyzer of Rohde & Schwarz ZVA8.

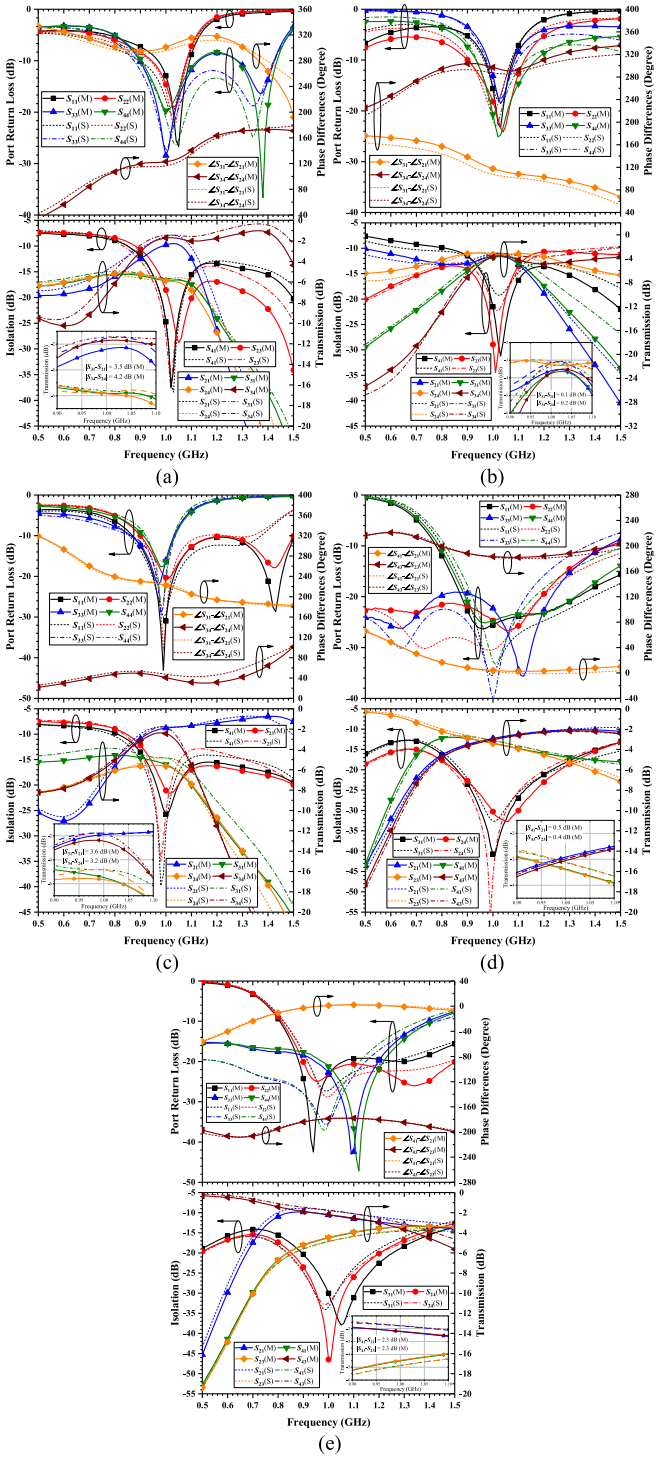

Fig. 6. Measured (M) and EM-simulated (S) S-parameters and phase differences. (a) *Case A*. (b) *Case B*. (c) *Case C*. (d) *Case D*. (e) *Case E*.

Fig. 6 shows the EM simulated and measured results of the five cases. Table III shows the bandwidth performances of the three cases (*A*, *B*, and *C*), where the measured data are in parentheses. The measured matching is all greater than 15 dB, and the isolation is all greater than 20 dB. Most of the deviations of the phase differences are less than $\pm 5°$ between the simulated and measured results. In *Case A* (4-dB), the power distributions at the two output ports are measured, 5.8 & 2.3 dB ($|S_{31}|$, $|S_{21}|$), 5.9 & 1.7 dB ($|S_{24}|$, $|S_{34}|$). Similarly, the

TABLE III
FRACTIONAL BANDWIDTH OF THE IDEAL CASE AND MEASURED MODEL (UNIT: %)

		*Case A**	*Case B**	*Case C**
Matching[1]	**10 dB**	23 (12)	18 (11)	13 (12)
	15 dB	11 (6)	10 (4)	7 (5)
Isolation: $\|S_{41}\|$	**15 dB**	22 (17)	18 (16)	23 (24)
	20 dB	12 (8)	10 (8)	11 (9)
Isolation: $\|S_{23}\|$	**15 dB**	22 (19**)	20 (16)	18 (21***)
	20 dB	12 (9)	10 (8)	9 (6)
Power Division 1[2]	**1 dB**	25 (16)	37 (28)	24 (13)
Power Division 2[3]	**1 dB**	30 (18)	21 (14)	28 (20)
Phase Difference 1[4]	**5°**	21 (6)	21 (10)	28 (8)
	2°	6 (4)	7 (4)	22 (3)
Phase Difference 2[5]	**5°**	25 (15)	23 (14)	57 (9)
	2°	7 (5)	16 (5)	10 (4)

[1]: $|S_{11}|\&|S_{22}|\&|S_{33}|\&|S_{44}|$ [2]: $|S_{31}|\&|S_{21}|$ [3]: $|S_{34}|\&|S_{24}|$ [4]: $\angle S_{31}$-$\angle S_{21}$ [5]: $\angle S_{34}$-$\angle S_{24}$
*: Values in parentheses are the measured data
: 17-dB fractional bandwidth *: 16-dB fractional bandwidth

TABLE IV
PERFORMANCE COMPARISON FOR THE COUPLERS

Ref.	**[1] (ex. 3)**	**[4] (Fig. 6)**	**[9] (Coupler 1)**	**[19]**	**This work (Case A)**
PD.	Arbitrary	Arbitrary	Arbitrary	Equal	**Arbitrary**
Load Impedances	I/O arbitrary	Identical	Identical	Not arbitrary	**Arbitrary**
Phase Difference	-180°-180°, rat-race included	-180°-180°, except 0° and 180°	-180°-180°, except rat-race	90°	**-180°-180°, rat-race included**
Band	Single	Single	Dual	Single	**Single**
Tech.	PCB	SMD	PCB	GaAs	**SMD**
Matching FBW. (%/dB)*	2 (20)	7.5 (15)	8.3/13.5 (20)	30.4 (20)	**6 (15)**
Iso. FBW. (%/dB)*	11 (20)	7 (20)	54.2/7.7 (20)	44.5 (20)	**8 (20)**
Phase Diff. Imbalance FBW. (%/°)*	18 (±2)	N/A	7.8/2.9 (±5)	17.4 (±2.5)	**4 (±2)**
PD. Deviation FBW. (%/dB)*	42 (±1)	N/A	14.1/7.4 (±1)	N/A	**16 (±1)**
Effective Size ($\lambda_g \times \lambda_g$)	0.31 × 0.13	0.03 × 0.04	0.42 × 0.16	0.04 × 0.02**	**0.06 × 0.06**

PD.: Power Division. Tech.: Technology. FBW.: Fractional Bandwidth. Iso.: Isolation.
*: only when port 1 is excited. **: when $\varepsilon_r = 12.9$. All values are measured results.

unequal power divisions at the two output ports are measured in *Case C* (3-dB), 5.5 & 1.9 dB, 5.6 & 2.4 dB, and *Case E* (3-dB), 4.5 & 2.2 dB ($|S_{41}|$, $|S_{21}|$), 4.5 & 2.2 dB ($|S_{23}|$, $|S_{43}|$). The equal power division is realized in *Case B* (3.7 & 3.6 dB, 3.5 & 3.3 dB) and *Case D* (3.4 & 2.9 dB, 3.0 & 3.4 dB). The deviation of the power-dividing ratio in these five cases is negligible, compared with the EM simulation results.

Overall, all the measured results agree well with the EM simulated results. The performance comparison for the couplers are shown in Table IV.

V. CONCLUSION

This brief proposed a compact coupler using eight LC elements which can implement arbitrary power-dividing ratios, arbitrary phase differences, and arbitrary terminated impedance matching. The close-formed design equations are derived and design procedure is listed including rat-race case. For verification, five instances are designed, simulated and fabricated. Good agreement between EM simulation and measurement validates the multifunctional coupler is of great advantageous in miniaturization and configuration simplicity.

REFERENCES

[1] Y. Wu, L. Jiao, Q. Xue, and Y. Liu, "A universal approach for designing an unequal branch-line coupler with arbitrary phase differences and input/output impedances," *IEEE Trans. Compon. Packag. Manuf. Technol.*, vol. 7, no. 6, pp. 944–955, Jun. 2017.

[2] Y. Wu, L. Jiao, Q. Xue, and Y. Liu, "Reply to 'comments on 'a universal approach for designing an unequal branch-line coupler with arbitrary phase differences and input/output impedances,'" *IEEE Trans. Compon. Packag. Manuf. Technol.*, vol. 9, no. 6, pp. 1210–1216, Jun. 2019.

[3] R. W. Vogel, "Analysis and design of lumped- and lumped-distributed-element directional couplers for MIC and MMIC applications," *IEEE Trans. Microw. Theory Techn.*, vol. 40, no. 2, pp. 253–262, Feb. 1992.

[4] E. Gandini, M. Ettorre, R. Sauleau, and A. Grbic, "A lumped-element unit cell for beam-forming networks and its application to a miniaturized butler matrix," *IEEE Trans. Microw. Theory Techn.*, vol. 61, no. 4, pp. 1477–1487, Apr. 2013.

[5] I. Sakagami, M. Tahara, and M. Fuji, "Lumped-element type D branch couplers," in *Asia Pac. Microw. Conf. Dig.*, Dec. 2009, pp. 2656–2659.

[6] Y. Zheng, W. Wang, and Y. Wu, "Synthesis of wideband filtering couplers for arbitrary high power-division ratios based on three different types of coupled-line sections," *IEEE Trans. Circuits Syst. II, Exp. Briefs*, vol. 68, no. 4, pp. 1218–1222, Apr. 2021.

[7] S. Y. Zheng, J. H. Deng, Y. M. Pan, and W. S. Chan, "Circular sector patch hybrid coupler with an arbitrary coupling coefficient and phase difference," *IEEE Trans. Microw. Theory Techn.*, vol. 61, no. 5, pp. 1781–1792, May 2013.

[8] L.-S. Wu, J. Mao, and W.-Y. Yin, "Miniaturization of rat-race coupler with dual-band arbitrary power divisions based on stepped-impedance double-sided parallel-strip line," *IEEE Trans. Compon. Packag. Manuf. Technol.*, vol. 2, no. 12, pp. 2017–2030, Dec. 2012.

[9] P.-L. Chi and K.-L. Ho, "Design of dual-band coupler with arbitrary power division ratios and phase differences," *IEEE Trans. Microw. Theory Techn.*, vol. 62, no. 12, pp. 2965–2974, Dec. 2014.

[10] I.-H. Lin, M. DeVincentis, C. Caloz, and T. Itoh, "Arbitrary dual-band components using composite right/left-handed transmission lines," *IEEE Trans. Microw. Theory Techn.*, vol. 52, no. 4, pp. 1142–1149, Apr. 2004.

[11] H. Liu, S. Fang, Z. Wang, and S. Fu, "Analysis and implementation of a dual-band coupled-line trans-directional coupler," *IEEE Trans. Circuits Syst. II, Exp. Briefs*, vol. 67, no. 3, pp. 485–490, Mar. 2020.

[12] W. Feng, Y. Zhao, W. Che, R. Gómez-García, and Q. Xue, "Multi-band balanced couplers with broadband common-mode suppression," *IEEE Trans. Circuits Syst. II, Exp. Briefs*, vol. 65, no. 12, pp. 1964–1968, Dec. 2018.

[13] X. Yi, Y. Shi, Z. Yu, and X. Qian, "Wideband and miniaturized forward-wave directional coupler using periodical parallel plates and vertical meander lines," *IEEE Trans. Circuits Syst. II, Exp. Briefs*, vol. 67, no. 11, pp. 2402–2406, Nov. 2020.

[14] A. M. Abbosh and M. E. Bialkowski, "Design of compact directional couplers for UWB applications," *IEEE Trans. Microw. Theory Techn.*, vol. 55, no. 2, pp. 189–194, Feb. 2007.

[15] A. M. Zaidi, B. K. Kanaujia, M. T. Beg, J. Kishor, and K. Rambabu, "A novel dual-band branch line coupler for dual-band butler matrix," *IEEE Trans. Circuits Syst. II, Exp. Briefs*, vol. 66, no. 12, pp. 1987–1991, Dec. 2019.

[16] F. Gong, C. Li, and J. DeGroat, "Analysis and design of a wide-band lumped-element quadrature directional coupler for complementary metal-oxide semiconductor implementation," *IET Microw. Antennas Propag.*, vol. 5, no. 4, pp. 443–449, Mar. 2011.

[17] O. Kazan, O. Memioglu, F. Kocer, A. Gundel, and C. Toker, "A lumped-element wideband 3-dB quadrature hybrid," *IEEE Microw. Wireless Compon. Lett.*, vol. 29, no. 6, pp. 385–387, Jun. 2019.

[18] X. Yu, and S. Sun, "Design of wideband lumped crossovers with resonator-loaded window shape structure," *IEEE Microw. Wireless Compon. Lett.*, vol. 29, no. 5, pp. 309–311, May 2019.

[19] T.-M, Shen, C.-R. Chen, T.-Y. Huang, and R.-B. Wu, "Design of lumped rat-race coupler in multilayer LTCC," in *Proc. Aisa Pac. Microw. Conf.*, Dec. 2009, pp. 2120–2123.

[20] H. Ahn, I. Nam, and O. Lee, "An integrated lumped-element quadrature coupler with impedance transforming," *IEEE Microw. Wireless Compon. Lett.*, vol. 30, no. 2, pp. 152–155, Feb. 2020.